CrossMark

RESEARCH ARTICLE

Recruitment of muscle synergies is associated with endpoint force fluctuations during multi-directional isometric contractions

Shota Hagio[1,2] · Motoki Kouzaki[2]

Abstract It has long been assumed that the human central nervous system uses flexible combinations of several muscle synergies to effortlessly and efficiently control redundant movements. However, whether muscle synergies exist in the neural circuit remains controversial, and it is critical to examine the association between the recruitment pattern of synergies and motor output. In this study, we examined the relationship between the activation of muscle synergies and endpoint force fluctuations in the presence of signal-dependent noise. Subjects performed multi-directional isometric force generations around the right ankle on the sagittal plane. We then extracted muscle synergies from measured electromyogram (EMG) data using nonnegative matrix factorization. As a result, the sum of the activation of muscle synergies was correlated with the endpoint force variability from the desired directions. Furthermore, we determined that the activation trace of each synergy reflected the endpoint force fluctuations using cross-correlation analysis. Therefore, these results suggest that muscle synergies statistically calculated from EMG data should be related to the motor output.

✉ Motoki Kouzaki
kouzaki.motoki.4x@kyoto-u.ac.jp

1 Japan Society for the Promotion of Science, Tokyo, Japan

2 Laboratory of Neurophysiology, Graduate School of Human and Environmental Studies, Kyoto University, Yoshida-Nihonmatsu-cho, Sakyo-ku, Kyoto 606-8501, Japan

Introduction

Individuals continually and effortlessly produce complicated movements, such as reaching for an object, that involve the control of an immense number of variables (Bernstein 1967). To simplify the control mechanisms of these movements, it has been suggested that the central nervous system (CNS) modularly organizes functionally similar muscles as several muscle synergies (Hagio and Kouzaki 2014; Tresch et al. 1999; d'Avella et al. 2003; Ting and Macpherson 2005). Task-dependent recruitment of muscle synergies has been examined in various tasks, such as reaching (d'Avella et al. 2006, 2008), postural response (Chvatal et al. 2011; Torres-Oviedo and Ting 2007, 2010) and isometric force generation in upper (Roh et al. 2012, 2013) and lower (Hagio and Kouzaki 2014) limbs. Although many researchers have addressed the identification of the neural structure of muscle synergies (Takei and Seki 2010; Hart and Giszter 2010), whether muscle synergies are of neural origin is controversial (Bizzi and Cheung 2013) and the existence of muscle synergies remains merely conjecture.

In the concept of muscle synergy, the CNS does not directly control the activation of a large number of muscles; instead, descending neural inputs (referred to as the "activation coefficient") to each muscle synergy are mainly controlled to produce the desired motor output. Hence, to specify the existence of muscle synergies, it is important to prove that the resulting motor output is modulated at the muscle synergy level rather than the individual muscle level by examining the relationship between the activation of statistically calculated muscle synergies and motor output. Some previous studies have demonstrated the correspondence between the activation of muscle synergies and endpoint force by reducing their dimensions

together (Chvatal et al. 2011; Ting and Macpherson 2005). Furthermore, the recent study suggested that a small set of muscle synergies could effectively control endpoint forces in a virtual environment based on the assumption that the activation of muscle synergies and endpoint forces were linearly related to each other (Berger and d'Avella 2014). Direct comparison between the activation of muscle synergies and endpoint force, however, is necessary to identify whether muscle synergies as a neural structure indeed contribute to generating endpoint force. It is well known that motor output includes the desired endpoint force and fluctuations in the presence of signal-dependent noise (SDN) (Harris and Wolpert 1998; Haruno and Wolpert 2005; Todorov and Jordan 2002), supposing that the motor command is corrupted by noise at the neuron level and that the amount of noise is scaled with the magnitude of the original motor command (Jones et al. 2002). A desired force reflects a high-level demand, whereas the endpoint force fluctuations derived from neural noise could comprehend the various information of the neural property at a lower level. Therefore, high-frequency force fluctuations will include the intrinsic properties of the relevant muscles, such as a line of action of muscle (Kutch et al. 2008) or neural control strategy (i.e., muscle synergies). In this study, we focused on high-frequency force fluctuations, including SDN, and experimentally examined the relationship with synergy activations.

The purpose of the present study was to reveal the association between the activation of muscle synergies and the high-frequency endpoint force variability in the presence of SDN. To accomplish our aim, subjects performed isometric multi-directional force generation around the ankle, and we quantified the relationship by two different comparisons: first, between the sums of synergy activations and the total force variability across the desired directions and second, between the time sequence of synergy activation and force traces. Our results demonstrated the association between neural activity and motor output based on the concept of muscle synergies and will lead to approaching the issue whether the CNS controls muscle synergies as the neural structure.

Materials and methods

Subjects

Ten male subjects voluntarily participated in this study. Their mean ($\pm$SD) age, height and body mass were 23.6 ± 0.52 years, 174.4 ± 3.6 cm and 66.8 ± 9.7 kg, respectively. All subjects were healthy, had no history of a neurological disorder and had corrected-to-normal vision. The subjects provided written informed consent to participate in

the study after they received a detailed explanation of the purposes, potential benefits and risks associated with participation. All procedures used in this study were in accordance with the Declaration of Helsinki and approved by the Committee for Human Experimentation at the Graduate School of Human and Environmental Studies, Kyoto University.

Experimental setup

The experiment comprised one component of our previous study (Hagio and Kouzaki 2014). The subjects laid on their left side on a bed with the right leg supported horizontally by a sling. The joint angles of both the knee and hip joints were 90° from full flexion. Isometric endpoint forces surrounding the right ankle were produced for a total of $\geq$10 s at two different intensities (20 and 40 N) in each of 12 different directions in the sagittal plane. The directions were equally distributed in 30° increments to cover the entire sagittal plane (Fig. 1a). We then measured the isometric endpoint forces, which were composed of two force vectors, F_x and F_y, which anatomically corresponded to knee flexion–extension and hip flexion–extension directions, respectively, using a triaxial force transducer (LSM-B-500NSA1, Kyowa, Tokyo, Japan) attached above the subject's right ankle (Kouzaki et al. 2002; Hagio et al. 2012) (Fig. 1b). To clarify the contribution of each joint torque to the generated endpoint force, we transported the endpoint forces into the knee flexion (T_k) and hip flexion (T_h) torques as follows:

$$\begin{pmatrix} T_k \\ T_h \end{pmatrix} = \begin{pmatrix} L_1 & 0 \\ -L_1 + L_2 \cos \alpha & L_2 \sin \alpha \end{pmatrix} \begin{pmatrix} F_x \\ F_y \end{pmatrix} \qquad (1)$$

where L_1 and L_2 represent the length between the lateral malleolus and the lateral epicondyle, and between the lateral epicondyle and the greater trochanter, respectively. α indicates the knee joint angle (90°). This equation was further translated into the following equation:

$$F_x = \frac{T_k}{L_1}, \quad F_y = \frac{T_k + T_h}{L_2}. \qquad (2)$$

If only the hip flexion or extension torque is active (i.e., $T_k = 0$, $F_x = 0$), the endpoint force is generated to 90° and 270° directions ($F_y = T_h/L_2$). If only the knee flexion or extension is active ($T_h = 0$), the force direction is (L_2, L_1); in a representative subject, the direction is approximately between 30° and 60° or between 210° and 240° because (L_2, L_1) is (42.0, 41.0 cm). In each trial, the subjects viewed the desired force as a target and endpoint force on a visual display.

Electromyography

Surface EMGs were recorded from the following 15 muscles that spanned the knee and hip joints: the rectus femoris (RF), vastus lateralis (VL), vastus medialis obliquus
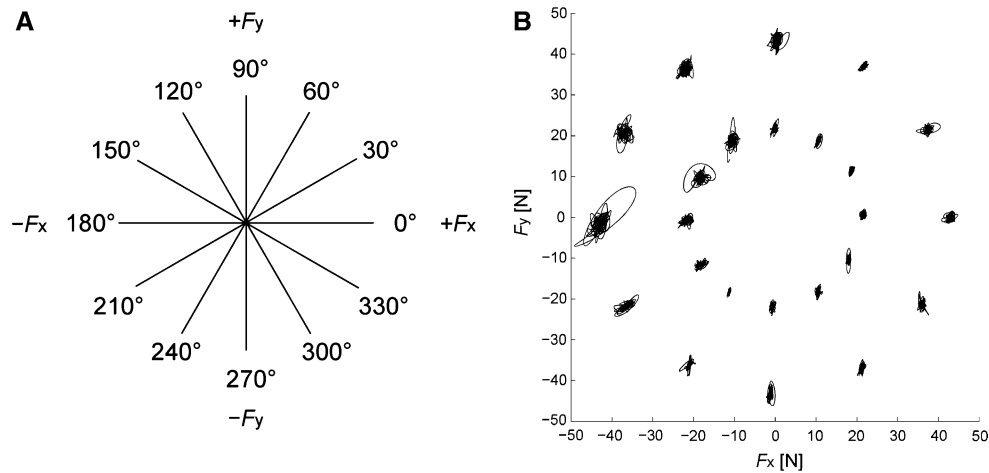
Fig. 1 Desired force direction and force trajectories. **a** Twelve target directions toward which isometric force generations were required. $+F_x$ and $+F_y$ corresponded to anatomical knee flexion and hip flexion directions, respectively. **b** Force trajectories across 12 force directions and two force levels in a representative subject are shown. The force traces were band-pass filtered at 8 and 30 Hz using a zero-phase-lag fourth-order Butterworth filter. For display purpose, each force trajectory was magnified five times

(VMO), vastus medialis longus (VML), vastus intermedius (VI), sartorius (SR), adductor longus (AL), biceps femoris long head (BFL), biceps femoris short head (BFS), semitendinosus (ST), semimembranosus (SM), gluteus maximus (GMax), gluteus medius (GMed), gastrocnemius lateralis (LG) and gastrocnemius medialis (MG). EMGs were recorded using bipolar Ag–AgCl electrodes. Each electrode had a diameter of 5 mm, and the inter-electrode distance was 10 mm (Hagio and Kouzaki 2014; Imagawa et al. 2013). We carefully obtained the site of electrode placement in each muscle with a B-mode ultrasonic apparatus (prosound α-6, Aloka, Tokyo, Japan) and used a small inter-electrode distance to prevent cross talk between neighboring muscles. A reference electrode was placed on the lateral epicondyle of femur. The EMG signals were amplified (MEG-6116M, Nihon Kohden, Tokyo, Japan) and band-pass filtered from 5 to 1000 Hz. All electrical signals were stored with a sampling frequency of 2000 Hz on the hard disk of a personal computer using a 16-bit analog-to-digital converter (PowerLab/16SP; AD Instruments, Sydney, Australia). The raw EMG traces were high-pass filtered at 35 Hz using a zero-phase-lag fourth-order Butterworth filter, after which they were demeaned, digitally rectified and low-pass filtered at 40 Hz (Chvatal et al. 2011). The filtered traces were then averaged across the hold period of each trial and across each corresponding deactivated rest period; the difference between the two traces served as the net EMG to eliminate noise at baseline. If some negative EMG responses exist, the negative value was replaced into 0, i.e., no activation. We eliminated the EMG traces during the first and last 1 s and analyzed the data for 8 s. The filtered traces were then divided into 100 time bins per 1 s and averaged across each bin (i.e., resampled at 100 Hz).

The muscle activity data for each muscle were assembled to form an EMG data matrix, which consisted of 15 muscles × 19,200 variables (12 directions × 2 force levels × 8 s × 100 time bins). The EMG values of each muscle were normalized to the maximum value for all muscles such that each value was between 0 and 1. Then, each muscle data vector was normalized to have unit variance to ensure the activity in all muscles was equally weighted.

Extraction of muscle synergies

We extracted muscle synergies from the data matrix of the EMG recordings using nonnegative matrix factorization (NMF) (Hagio and Kouzaki 2014; Lee and Seung 1999; Ting and Macpherson 2005; Tresch et al. 1999). The construction of a muscle activation pattern (M) evoked to achieve an isometric endpoint force in a particular direction was modeled with the following equation:

$$M = \sum_{i=1}^{N} W_i C_i + \varepsilon \quad (W_i \geq 0, \ C_i \geq 0)$$

where W_i represents the contribution of each muscle to synergy i, and an individual muscle may contribute to multiple synergies. The composition of the muscle synergies does not change between the conditions, but each synergy is multiplied by a scalar activation coefficient (C_i) that does change between conditions: the column of C_i consisted of 19,200 variables (12 directions × 2 force levels × 8 s × 100 time bins). ε is residual. The synergy weighting and activation coefficient matrices were normalized such that the individual muscle-weighting vector was the unit vector.

To select the number of muscle synergies that could best model our data, we extracted between 1 and 15 synergy matrices and synergy activation coefficient matrices from the EMG data matrices that were obtained from each subject. We subsequently verified the goodness of fit between the original (EMG$_o$) and reconstructed (EMG$_r$) data matrices; the data matrices were calculated using NMF analysis to select the smallest number of muscle synergies (N_{syn}) that resulted in an adequate reconstruction of the muscle responses. We first calculated the variability that accounted for (VAF) as $100 \times$ the coefficient of determination from the uncentered Pearson correlation coefficient (Torres-Oviedo et al. 2006; Zar 1999), which was based on the entire dataset (global VAF). The number of muscle synergies underlying each dataset was defined as the minimum number of synergies required to achieve a mean global VAF >90 % and a mean VAF for each muscle (muscle VAF) that exceeded 80 %. For N_{syn} muscle synergies, both synergy weighting and synergy activation coefficient matrices were defined.

Grouping of similar muscle synergies across subjects

Functional sorting of the global synergies across each subject was initially performed by grouping muscle synergies based on the values of cosine similarity ($r > 0.60$; $p < 0.01$) to that of an arbitrary reference subject using an iterative process (Hagio and Kouzaki 2014). If two synergies in one subject were assigned to the same synergy group, we defined a pair of synergies with the highest correlation as the same group of synergies. Subsequently, an averaged set of similar muscle synergies for all subjects was computed, and the similarity between the averaged muscle synergies and each synergy grouped across the subjects was quantified (Torres-Oviedo and Ting 2007).

Quantification of total force fluctuations

The force variability across the desired directions was quantified using target-directed variance (η), which indicates the degree to which the covariance for each trial was aligned with the desired force direction of that trial (Imagawa et al. 2013; Kutch et al. 2008). We focused on high-frequency force variability, which measured the anatomical features inherent in the individual muscles such as a line of action. The target-directed variance reflects the contribution of muscles (muscle synergies) to the desired direction as a prime mover or the combination of different muscles (or muscle synergies) having divergent action directions. We first cropped each trial to isolate the relatively constant forces that were generated for duration of 8 s. The time series of the force vectors, $F_x(t)$ and $F_y(t)$, were combined into a vector time series [$F(t)$]. The empirical target force vector F_{target} was defined as the equivalent

to the average force vector $\bar{F}$, and $\hat{F}_{target}$ was defined as the unit vector in a given direction. The force data were band-pass filtered at 8 and 30 Hz. The filtered force data $\tilde{F}$ were then used to compute the force covariance. We referred to the covariance matrix of filtered forces as cov[$\tilde{F}$], thus

$$\eta = \frac{\hat{F}_{target}^T \text{cov}\left[\tilde{F}\right] \hat{F}_{target}}{\text{Trace}\left\{\text{cov}\left[\tilde{F}\right]\right\}}$$

where the numerator quantifies the amount of variance that occurred in the target direction and the denominator summarizes the total amount of variance as a scalar. If the force variability on the sagittal plane was aligned with the desired force direction, the η value shows 1; if not, the η value approaches 0.

To emphasize the target-directed dependence of the target-directed variance value, we also estimated the nontarget-directed force variance (so-called variance), which was calculated as the total variance (Trace{cov[$\tilde{F}$]}). For display purposes, the nontarget-directed variance values were normalized to the maximum across all subjects.

Comparison between activation of muscle synergies and force variability

To examine the relationship between the activation of muscle synergies and motor output, we first evaluated whether the characteristics of the high-frequency force variability related to the desired activation of the extracted muscle synergies across the target directions. To this end, we calculated Pearson's correlation coefficients (r_p) between the sum of all activation coefficients of the muscle synergies and the η value across the target directions. The summations of all activation coefficients were normalized to the maximal value across the force levels. For comparison, we also evaluated the relationships between the sum of the activation coefficients of the synergies and the nontarget-directed variance normalized to the maximum.

Correlation between activation of muscle synergies and force fluctuations

To evaluate whether the activation of muscle synergies reflected the high-frequency force fluctuations, we estimated a cross-correlation of activation traces of individual muscle synergies and two force signals (F_x and F_y). This analysis was performed over an approximately steady period of force fluctuations that lasted 8 s out of the time course. Each correlation coefficient trace was quantified based on a time lag from 0 to 200 ms. The correlation coefficient traces, in which time to peak values were physiologically meaningful, i.e., the synergy activation preceded

the resulting force between 0 and 200 ms (Vos et al. 1990 in the case of muscles), and in which the peak values were statistically different from zero ($r > 0.195$; $p < 0.05$, $n = 800$ [8 s × 100 time bins]; Masani et al. 2003), were adopted. We first assembled the correlation coefficient traces across similar groups of synergies for all subjects, directions and force levels. The positive and negative values indicated the correlation with anatomical flexion and extension forces, respectively. Correlation coefficients (C_r) were defined as the peak value of the correlation coefficient traces. The average value of the correlation coefficients was obtained across the traces representing positive (C_{rp}) and negative (C_{rn}) peak. We furthermore calculated the average peak value of the correlation coefficient traces across the desired force directions to examine in which force direction the correlation was observed. The averaging was estimated across two force vectors (F_x and F_y) and across positive and negative correlations within the population that the correlation could take. The value was then normalized with the maximal value for all correlation coefficients after the averaging. To clearly understand the features of the correlations across the directions, 12 averaged correlation coefficients across the directions were interpolated into 200 points.

Results

Quantification of endpoint force variability

The endpoint force variability was quantified as the *target-directed variance*, which represents the extent of high-frequency force variability from the given target direction (Fig. 2a). Anatomical knee flexion and extension directions exhibited low target-directed variance (e.g., for 0°, 150°, 180° and 330°, the index values of the target-directed variance (η) were 0.35 ± 0.14, 0.35 ± 0.10, 0.40 ± 0.12 and 0.35 ± 0.13, respectively; Table 1). These findings indicate that the force trajectories were relatively broad and poorly aligned with the target direction. Conversely, high η values were identified in the anatomical hip flexion and extension directions (e.g., the η values for 90° and 270° were 0.82 ± 0.08 and 0.891 ± 0.033, respectively; Table 1) and 60° and 240° directions (η values were 0.77 ± 0.05 and 0.87 ± 0.06, respectively; Table 1), indicating that these force trajectories were narrow and well aligned with the target direction. Interestingly, the standard deviations for individual subjects and intensities were especially low. Figure 2b shows the nontarget-directed variance. The variances tended to be higher in the anatomical knee extension directions (e.g., the variance of 180° was 0.49 ± 0.27; Table 1) than the other directions, and the profile was different from the target-directed variance. The standard deviations were remarkably higher than in the case of target-directed variance, regardless of the target direction.

Muscle synergies

To examine the synergies around hip and knee joints, the subjects were instructed to exert endpoint isometric forces on a sagittal plane. We decomposed surface EMG data measured from 15 muscles, and approximately seven synergies across subjects were required for good reconstruction
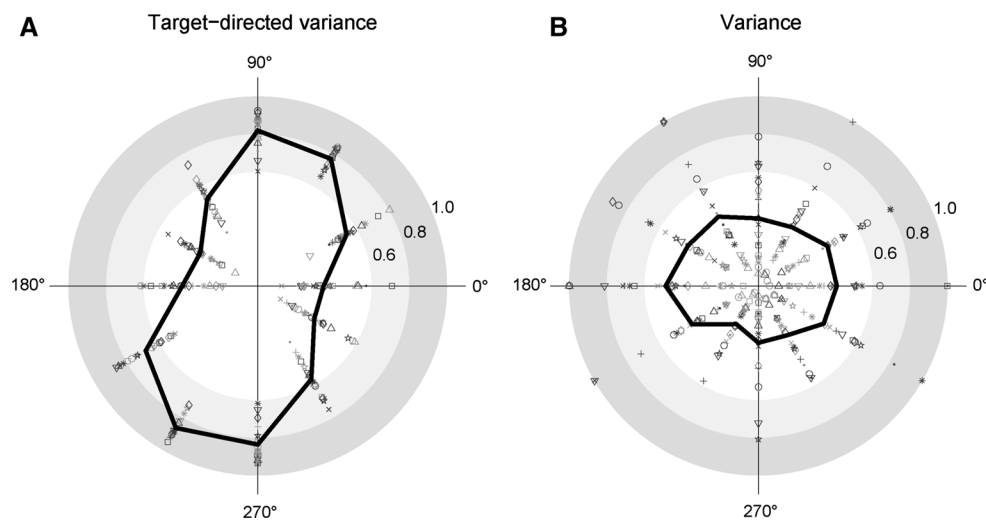
Fig. 2 Target- and nontarget-directed variance for the each target direction. Relationships between the endpoint force variability and the target force direction were quantified across target directions by **a** the target-directed variance (η) and **b** nontarget-directed variance. Different target magnitude 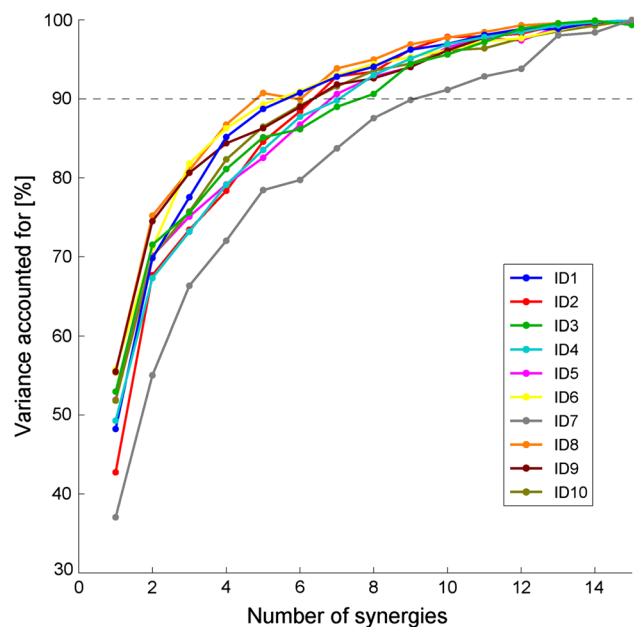levels are represented by *different colors*, whereas different subjects are represented by *different symbols*. In the case of the nontarget-directed variance, the values were normalized to the maximum across the subjects. A *thick curve* represents the average across the subjects and the target levels within each 30° bin of the target direction

Table 1 Target-directed variance (η) and nontarget-directed variance across the desired force directions

	Index	0°	30°	60°	90°	120°	150°	180°	210°	240°	270°	300°	330°
Target-directed variance (η)	Average	0.349	0.543	0.775	0.820	0.533	0.350	0.399	0.684	0.866	0.838	0.568	0.345
	SD	0.139	0.104	0.053	0.083	0.095	0.099	0.124	0.116	0.060	0.098	0.103	0.126
Nontarget-directed variance	Average	0.416	0.422	0.358	0.357	0.422	0.428	0.490	0.405	0.233	0.300	0.301	0.399
	SD	0.250	0.214	0.221	0.208	0.258	0.205	0.266	0.247	0.135	0.210	0.158	0.249

Average and standard deviation of η and variance values are shown across target directions. These average values correspond to the averages that are represented by a thick curve in Fig. 2

based on the criteria (global VAF >90 %, muscle VAF >80 %) (Fig. 3). Figure 4 displays the seven synergies (left) and the associated activation coefficients (right), which were an average of the activation traces for 8 s, in a representative subject. The first synergy primarily consisted of a bi-articular knee extensor and hip flexor (RF) and contributed to the knee extension and hip flexion torques (approximately 180°). The second synergy, which contained mono-articular knee extensors (VL, VML, VMO and VI), highly contributed to the 240° direction, i.e., the knee extension torque generation. The third synergy was dominated by the activation of the SR, which was activated in the knee and hip flexion direction approximately 60°. The fourth synergy, which was mainly composed of ST and SM, contributed to the force in the directions of knee flexion. The

fifth knee flexor and hip extensor synergy constructed by BFL and BFS were activated approximately 300° and 330° directions. These synergies were directionally tuned in the sagittal plane and had their preferred activation directions. The sixth and seventh synergies, which were composed of gluteus muscles (GMax and GMed) and LG, respectively, were broadly activated to maintain the desired direction.

Association between the activation of muscle synergies and target-directed variance

To investigate the relationship between the high-frequency endpoint force variability from the required target directions and the activation coefficients of muscle synergies, we compared the averaged index values of the target-directed variance (η) and the sum of the activation coefficients of all of the synergies averaged for all subjects (Fig. 5). We identified a significant negative correlation between these variables ($r = -0.47$, $p < 0.01$), which indicates the existence of a correlation between the synergy activation coefficient and the endpoint force variability from a desired target direction. For the individual subjects, significant strong correlations were identified in 6 of 10 subjects ($r = -0.61$, $r = -0.62$, $r = -0.56$, $r = -0.81$ and $r = -0.69$; $p < 0.01$ and $r = -0.41$; $p < 0.05$), and high correlation was observed in one subject (-0.40; $p = 0.054$). This result indicated the relationship between the characteristics of force variability and total desired activation of muscle synergies across the target directions.

Similarity of muscle synergies across subjects

We extracted 7.1 ± 1.37 muscle synergies across the subjects and grouped them into 11 groups of similar synergies (W_{1-11}) and four subject-specific synergies (Fig. 6). The synergy W_1, which mainly contained RF, was highly similar among all subjects ($r > 0.96$). The synergies W_2 composed of VL, VML, VMO and VI; W_4 constructed by ST, SM and MG; and W_6, which predominantly included GMax, were also similar among almost all subjects ($r > 0.71$, $r > 0.59$ and $r > 0.53$, respectively). The synergies W_3, W_5, W_7 and W_8, which were primarily constructed by SR, BFL, LG and

Fig. 3 Variance accounted for in the data reconstruction. The goodness of data reconstruction quantified by the global VAF (variance accounted for) as a function of the number of global synergies across the subjects is shown. Different subjects are represented by *different colors*. The number of muscle synergies was determined as the lowest number of synergies that achieved a mean global VAF >90 % (*solid line*) and a mean VAF for each muscle (muscle VAF) >80 %

Fig. 4 Muscle synergies and their activation coefficients. Muscle synergies (*left*) and their activation coefficients (*right*) across desired force directions in the force level of 20 N, which were extracted from the EMG data matrix using nonnegative matrix factorization (NMF), are shown for one representative subject. Each muscle-weighting vector of muscle synergies was normalized to represent the unit vector. The activation coefficients were averaged for 8 s across the force directions. A *value in the figure of the synergy activation* represents the *scale* at the edge of the *dashed circle*. *Muscle names* are indicated in an abbreviated form. *RF* rectus femoris, *VL* vastus lateralis, *VMO* vastus medialis obliquus, *VML* vastus medialis longus, *VI* vastus intermedius, *SR* sartorius, *AL* adductor longus, *BFL* biceps femoris long head, *BFS*, biceps femoris short head, *ST* semitendinosus, *SM* semimembranosus, *GMax* gluteus maximus, *GMed* gluteus medius, *LG* gastrocnemius lateralis, *MG* gastrocnemius medialis
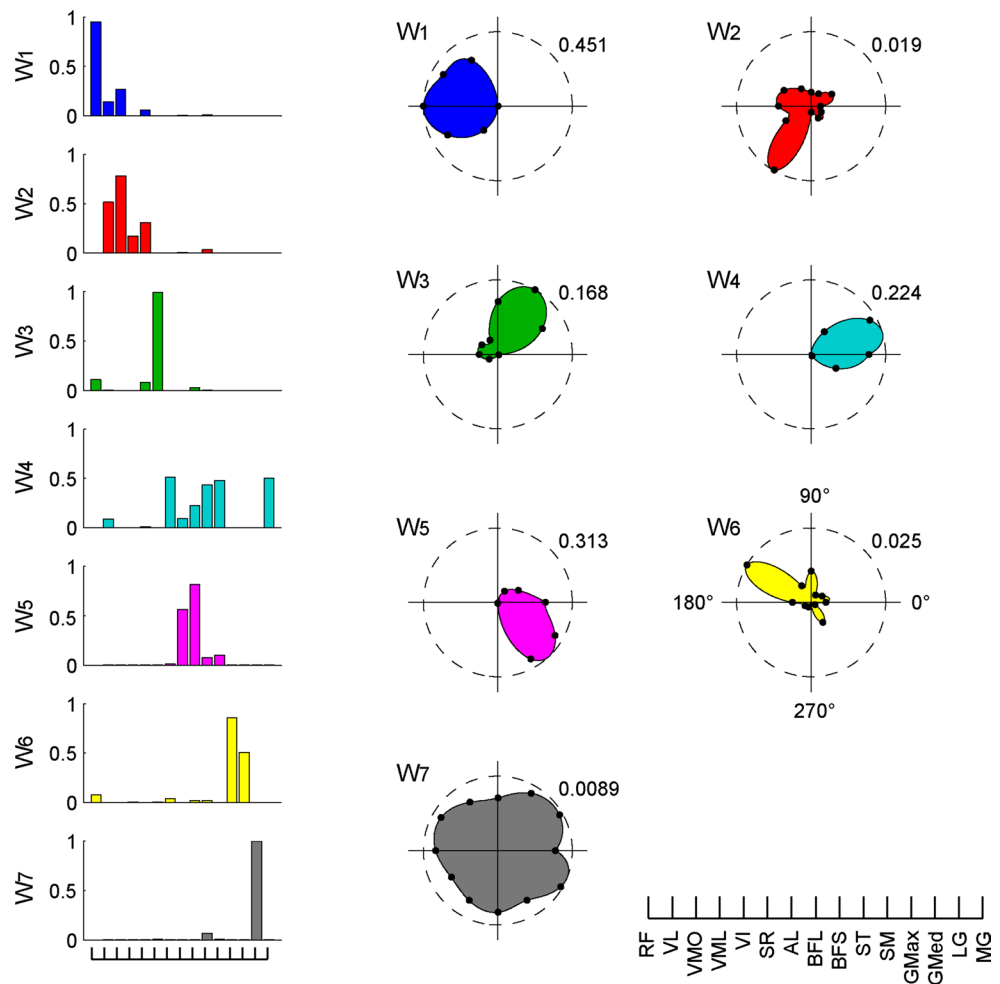

MG, respectively, were similar among approximately half of all subjects. ($r > 0.84$, $r > 0.56$, $r > 0.83$ and $r > 0.68$, respectively). The synergies W_9 included GMed; W_{10} having VL; and W_{11} constructed by VML were observed in two subjects. Moreover, four subjects had subject-specific synergies, which were not similar to any synergies in the other subjects.

Cross-correlation between synergy activations and force fluctuations

We examined the contribution of each synergy activation to the desired endpoint force by calculating the relationship between the synergy activation traces and the force fluctuations using a cross-correlation analysis. Figure 7 shows the correlation coefficient traces between two force vectors [F_x (middle) and F_y (bottom)] and the synergy activations in six groups of similar synergies across the subjects (W_{1-6} in Fig. 6). The correlation coefficient traces were adopted because the peak value exceeded 0.195 (i.e., significant), and the time to peak value was physiologically meaningful (see "Materials and methods" section). The displayed

synergies (top) represent the average of the same synergy group in Fig. 6. Furthermore, the peak values of the correlation coefficient traces were averaged across the force directions to examine in which desired force direction the correlation was observed (Fig. 8). The activation of the synergy W_1 had a significant negative correlation with F_x ($C_{rxn} = -0.227$) around 180°. This synergy also correlated with F_y ($C_{ryn} = -0.153$) in between 180° and 210°. The activation of the synergy W_2 was correlated with F_x both positively ($C_{rxp} = 0.170$) at approximately 30° and in between 300° and 330° and negatively ($C_{rxn} = -0.182$) near 210°. The synergy W2 also showed negative correlation with F_y ($C_{ryn} = -0.156$) around 210°. In the synergy W_3, both positive and negative correlations with F_x were observed at approximately 30° and 180°, respectively ($C_{rxp} = 0.185$ and $C_{rxn} = -0.168$, respectively). This synergy was also significantly associated with F_y ($C_{ryp} = 0.240$) at approximately 60°. The activation of synergy W_4 was significantly correlated with F_x ($C_{rxp} = 0.233$) at approximately 0°. In the synergy W_5, the activation was positively correlated with both F_x ($C_{rxp} = 0.218$) and F_y ($C_{ryp} = 0.200$) at approximately 0° for both values. The
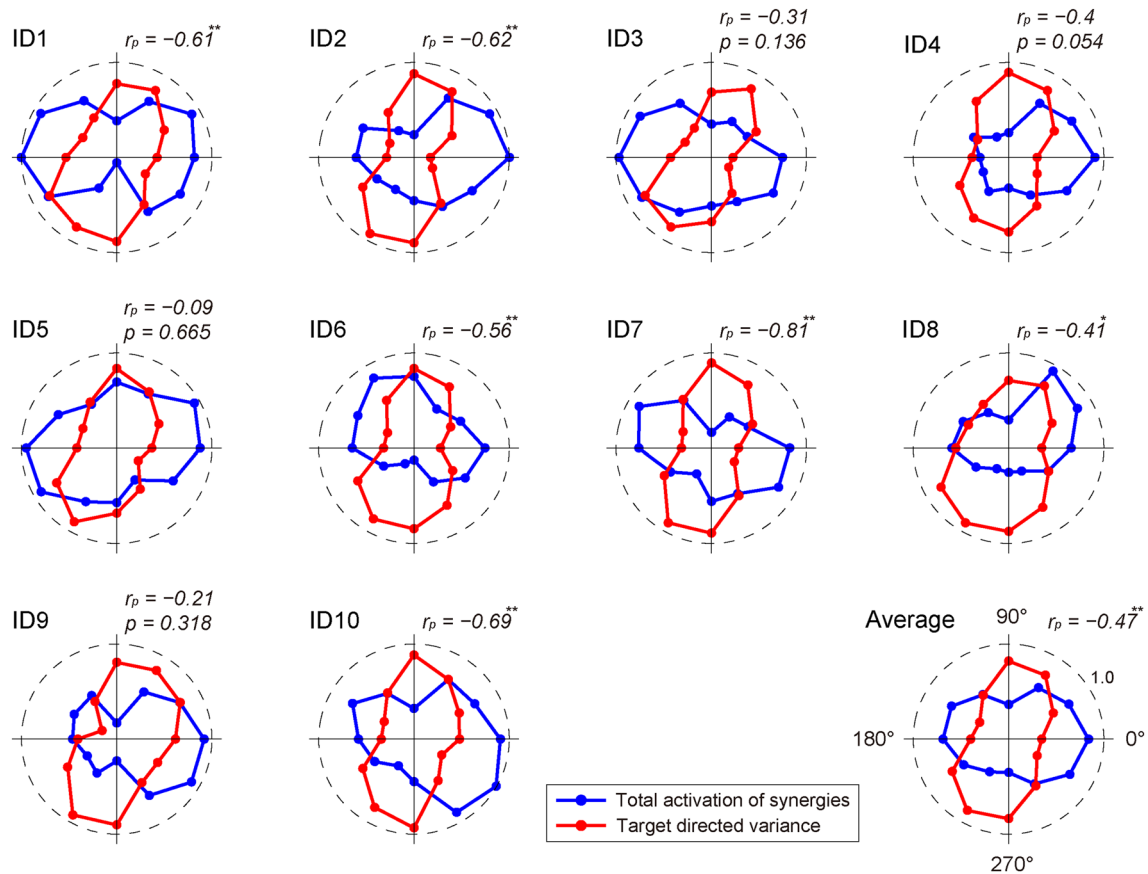
Fig. 5 Relationship between the target-directed variance and the sum of the activation coefficient of the muscle synergies. Relationships between the η value (*red*) and the sum of the activation coefficients of the muscle synergies (*blue*) across subjects and for all subjects are shown (*$p < 0.05$; **$p < 0.01$)

activation of the synergy W_6 had positive correlation with F_x and F_y ($C_{rxp} = 0.215$ and $C_{ryp} = 0.156$, respectively) around some directions. These results denoted that the activation traces of muscle synergies reflect the force output.

We then estimated the time to peak value of the correlation coefficient traces, which represent the time lag from the activation of each synergy to the resulting endpoint force, i.e., the electromechanical delay (EMD) (which were exactly at the level of muscle translated into the structure of muscle synergies using dimensional reduction). Figure 9 shows the distribution of the time to peak value in the correlation with both F_x (gray) and F_y (black) as histograms. In all synergies, the time to peak values were distributed at approximately 100 ms [95.89, 86.14, 96.50, 94.10, 95.41, 101.82 and 112.50 (ms) in W_{1-6}, respectively].

Discussion

The main purpose of the present study was to examine the association between the activation of muscle synergies and the high-frequency endpoint force variability in the

presence of SDN. To accomplish this aim, we extracted muscle synergies from the femoral region; approximately seven synergies across subjects were determined. The high-frequency force variability from the desired target directions was first quantified as the target-directed variance (η), and we identified a negative correlation between the sum of the activations of muscle synergies and the target-directed variance. Second, we estimated the relationship between the high-frequency fluctuations and the activation traces of the individual synergies and observed a significant correlation between them. These results indicated that the activation of muscle synergies correlated with motor output.

One of the main findings in the present study was a high correlation between the η values and the sum of the activation coefficients of the muscle synergies (Fig. 5). For example, the directions of 60°, 90°, 240° and 270° had high η values, which were above or near 0.8 (Fig. 2; Table 1), and the sum of the synergy activations was relatively low. The fraction of the target-directed variance was characterized by a combination of relevant muscles; for directions in which the application is accomplished by muscles that have similar action directions, the η value is
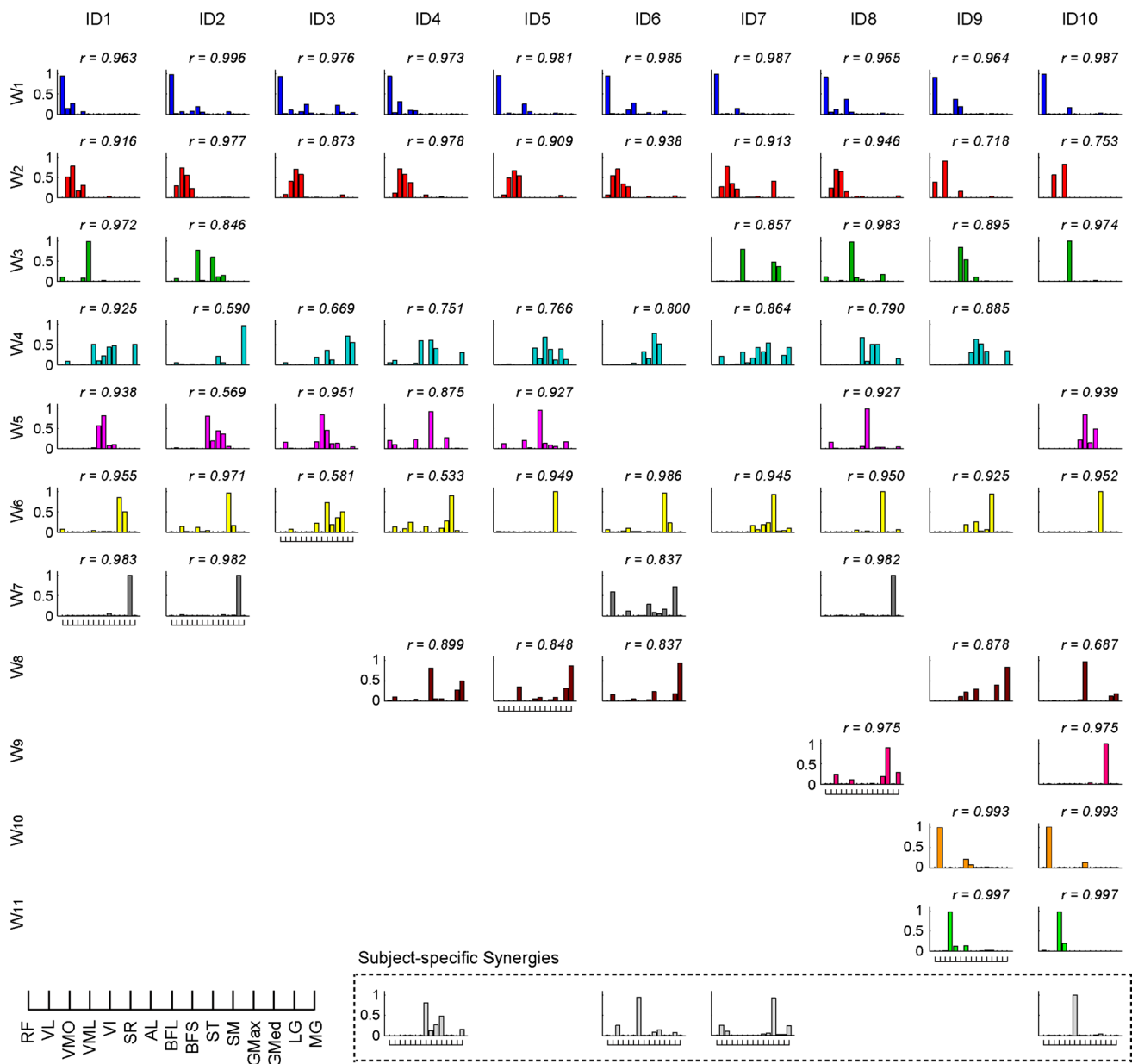
Fig. 6 Muscle synergies for all subjects. The muscle weightings of the muscle synergies of each subject are shown. The *r* value represents cosine similarities between the averaged muscle synergies from the initial sorting and each original synergy grouped across the sub- jects (see "Materials and methods" section). All the *r* values are statistically significant, i.e., $r > 0.6$ and $r > 0.5$ ($p < 0.01$ and $p < 0.05$, respectively). The synergies across the subjects were grouped into 11 groups and four subject-specific synergies

high, whereas the combinations of muscles that have different action directions are reflected by a low η value (Kutch et al. 2008). Hence, one or more muscles that have a similar action direction generated the forces to these directions. In the directions of 90° and 270°, only the hip flexion and extension torques were required to generate the endpoint force (Eq. 2). Near the 60° and 240° directions, the knee flexion and extension torques predominantly contributed to the force production. Therefore, regarding the concept of muscle synergies, the target-directed variance in these

directions might be attributed to the contribution of the muscle synergies, which independently worked on the relevant joint (e.g., W_6 in Fig. 6) or which were constructed by the muscles that had a similar action direction to the direction (e.g., W_2 in Fig. 6). Conversely, the other directions, especially 0°, 30°, 150°, 180° and 210°, had low η values. In these directions, the endpoint forces could be produced by the combinations of some muscle synergies or by the synergies composed of the muscles that had different action directions. These results suggest that the CNS required
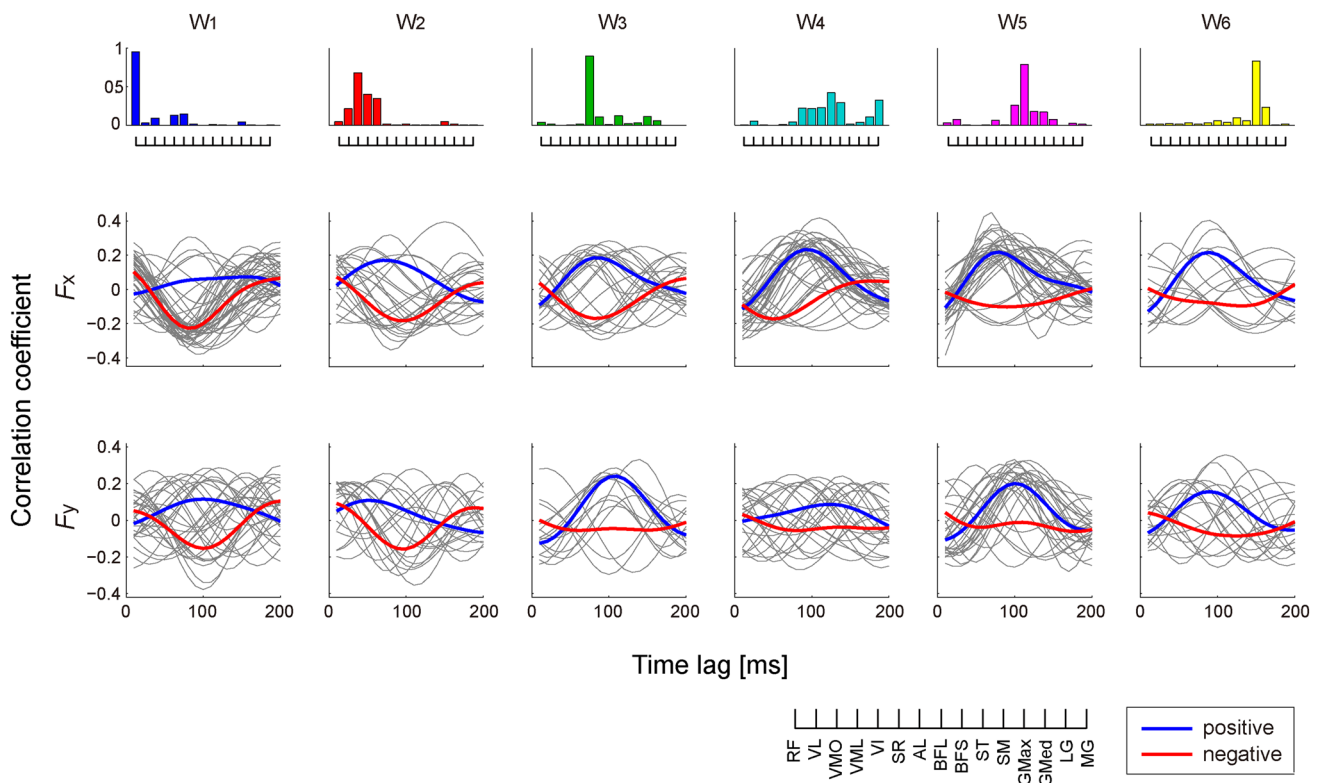
Fig. 7 Correlation between traces of synergy activations and force fluctuations. *Top* averaged muscle synergies across the same synergy group $W_{1–6}$ in Fig. 6. *Middle* and *bottom* correlation coefficient traces between the two force vectors (F_x and F_y) and synergy activations in six groups of similar synergies across trials. Each of the *gray* traces was obtained by cross-correlation analysis across each pair between force fluctuations and synergy activations. The correlation coefficient traces were adopted because the peak value exceeded 0.195 (i.e., significant) and the time to peak value was physiologically meaningful (see "Materials and methods" section). The correlation coefficient traces were averaged across traces, which represents positive (*blue*) and negative (*red*) peak correlations

relatively low activation of the synergy, which contributed to the desired force direction as the prime mover. In contrast, the force, in which the direction has no prime moving synergies and requires the combination of several synergies, was achieved by sending relatively large signals to the relevant synergies. Additionally, the variability of the η values across subjects was remarkably low, whereas the nontarget-directed variances were variable within the individual subjects, which indicates that the high-frequency variability from a target direction depends on some anatomical constraints inherent in our motor system. Therefore, the correlation between the sum of the synergy activations and this variability suggests that the intrinsic property of the musculoskeletal system should mainly determine the structures of muscle synergies and their modulation. This idea was ensured by the similarity of muscle synergies across subjects (Fig. 6; Torres-Oviedo and Ting 2010).

We then examined the contribution of each synergy to the endpoint forces by using the cross-correlation analysis between synergy activation and force fluctuations. All synergies were significantly correlated with both or one of two forces that corresponded to the relevant force direction of the muscles, which constructed the synergies (Fig. 7). Several synergies, however, had a correlation with a force in the direction that was not intuitively corresponding to the anatomical contribution. For example, the synergies W_1 and W_2 were associated with the force, $-F_y$, although the synergies anatomically contributed to the forces both in the knee extension ($-F_x$) and hip flexion ($+F_y$) directions and only in the knee extension direction ($-F_x$), respectively. This result would arise from a higher correlation with the knee extension torque because both the knee extension and hip extension torques contribute to $-F_y$ (Eq. 2). Furthermore, the activations of all synergies correlated with both positive and negative force vectors, i.e., not only the directly relevant force but also the opposite force direction. We speculated that these correlations with anatomically opposite directions were attributed to the low activations of the relevant muscles, which were observed in the low contribution to the opposite torque (Jacobs and van Ingen Schenau 1992). These opposite correlations were present in the force generations against the directly relevant directions (Fig. 8), for example, between 30° and 60°, and between 300° and 330° in W_2.
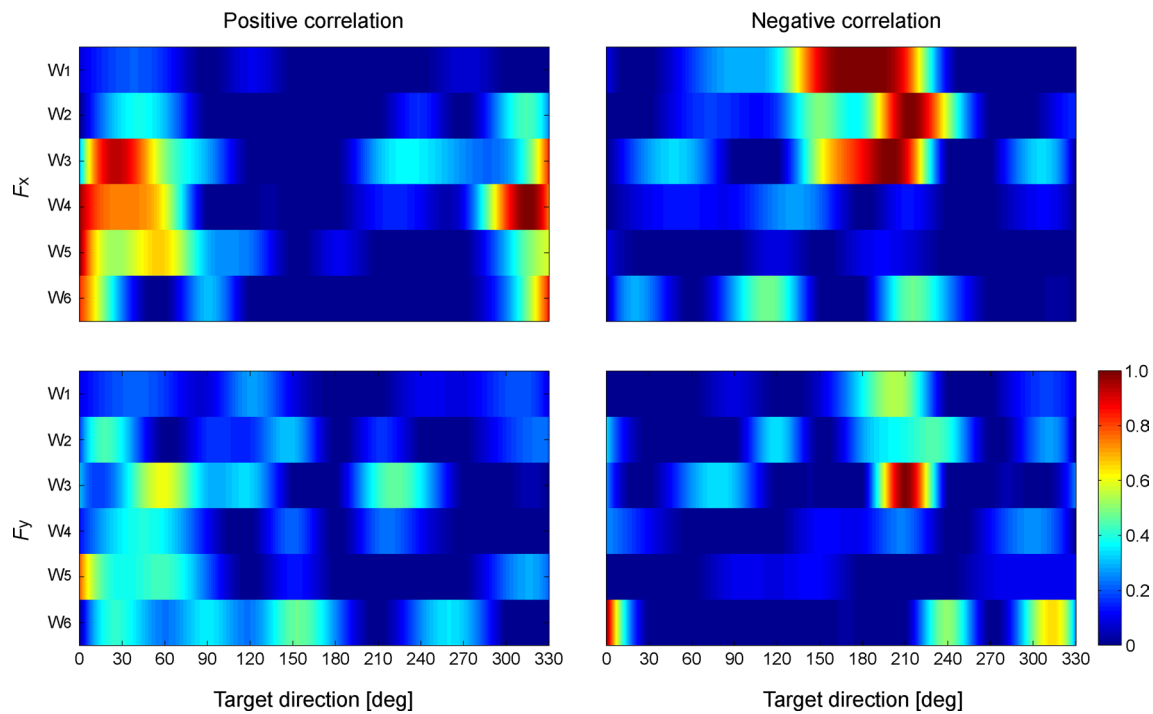
Fig. 8 Correlation coefficients across the desired force directions. Absolute values of the correlation coefficients between the synergy activations and the force fluctuations across the desired force directions are shown. The correlation coefficients represented averages of the peak absolute values in each correlation coefficient trace within the same group of the synergies across two force vectors (F_x and F_y)

and across positive and negative correlations. The value was normalized with the maximal correlation coefficients. To obtain a clear understanding, 12 averaged correlation coefficients across the directions were interpolated into 200 points. The synergies W_{1-6} corresponded to the synergies in Fig. 6
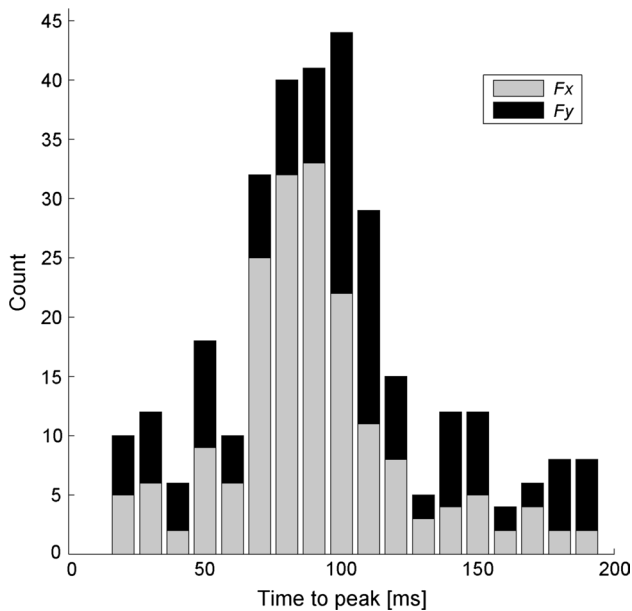
Fig. 9 Time to peak value of the correlation coefficient traces. Histogram of the time to peak value in the correlation coefficient traces, which represents the time lag from the activation of each synergy to the resulting endpoint force, is shown in the correlation with both F_x (*gray*) and F_y (*black*). The time to peak value was normally distributed at approximately 100 ms

The critical question is whether muscle synergies are of neural origin (Bizzi and Cheung 2013). A critique of the muscle synergy hypothesis is that it does not reflect neural structure but merely co-activation of functionally similar muscles or motor execution based on other criteria such as optimal control (Kurtzer et al. 2006; Tresch and Jarc 2009). Thus, muscle synergies are the secondary product that results from the analysis of EMG datasets using a decomposition technique [e.g., NMF (Lee and Seung 1999; Tresch et al. 1999) and independent component analysis; ICA (Hart and Giszter 2004, 2010)]. Recent studies, however, have provided evidence to support the existence of muscle synergies by examining the relationship between spinal interneurons and muscles. Takei and Seki (2010) demonstrated that premotor interneurons modularly control intrinsic hand muscles in monkeys by compiling spike-triggered averages of rectified EMGs for each interneuron (Takei and Seki 2010). Hart and Giszter (2010) demonstrated postspike facilitation effects on muscle responses for spinal interneurons in frogs and that the facilitation matched the weighting parameters of the individual primitives (referred to as muscle synergies in the present study) extracted via statistical analysis (Hart and Giszter 2010). Thus, these findings suggest that muscle synergies are in the spinal region as

interneurons. In this study, we addressed the verification of muscle synergies using different approaches, i.e., examination of the correlation between force fluctuations and activation of statistically calculated muscle synergy. The previous studies revealed the contribution of each muscle synergy to motor behavior, such as the endpoint force or the center of mass acceleration in the postural response (Chvatal et al. 2011; Ting and Macpherson 2005). However, these studies addressed the characteristics of a low-dimensional system, which was sometimes regarded as biomechanical constraints (Kutch and Valero-Cuevas 2012), rather than the neural structure of muscle synergies. Our results implied that the endpoint force fluctuations reflect the SDN fluctuations at the intermediate neurons as muscle synergies. Hence, muscle synergies that result from statistical calculations represented not only the co-activation of several muscles but also the neural structure that modularly organizes multiple muscles, which contributed to the force output. Therefore, the CNS may primarily control the endpoint force at the muscle synergy level rather than at the muscle level and reduce the high degree of freedom. The existence of muscle synergies, however, remains controversial. Thus, further studies must examine the detailed neural structure or functional meanings of muscle synergies.

In summary, we demonstrated that during isometric contractions related to the hip and knee joints, there was a significant negative correlation between the high-frequency force variability from the desired target directions and the sum of the activation of muscle synergies. The activations of the individual muscle synergies were significantly correlated with force fluctuations. These results suggest that the CNS modulates the endpoint force at the muscle synergy level rather than the muscle level and imply the existence of muscle synergies in the neural circuit.

References

Berger DJ, d'Avella A (2014) Effective force control by muscle synergies. Front Comput Neurosci 8(46):1–13

Bernstein N (1967) The coordination and regulation of movements. Pergamon Press, New York

Bizzi E, Cheung VCK (2013) The neural origin of muscle synergies. Front Comput Neurosci 7(51):1–6

Chvatal SA, Torres-Oviedo G, Safavynia SA, Ting LH (2011) Common muscle synergies for control of center of mass and force in nonstepping and stepping postural behaviors. J Neurophysiol 106:999–1015

d'Avella A, Saltiel P, Bizzi E (2003) Combinations of muscle synergies in the construction of natural motor behavior. Nat Neurosci 6(3):300–308

d'Avella A, Portone A, Fernandez L, Lacquaniti F (2006) Control of fast-reaching movements by muscle synergy combinations. J. Nerosci 26(30):7791–7810

d'Avella A, Fernandez L, Portone A, Lacquaniti F (2008) Modulation of phasic and tonic muscle synergies with reaching direction and speed. J Neurophysiol 100:1433–1454

Hagio S, Kouzaki M (2014) The flexible recruitment of muscle synergies depends on the required force-generating capability. J Neurophysiol 112(2):316–327

Hagio S, Nagata K, Kouzaki M (2012) Region specificity of rectus femoris muscle for force vectors in vivo. J Biomech 45:179–182

Harris CM, Wolpert DM (1998) Signal-dependent noise determines motor planning. Nature 394:780–784

Hart CB, Giszter SF (2004) Modular premotor drives and unit bursts as primitives for frog motor behaviors. J Neurosci 24(22):5269–5282

Hart CB, Giszter SF (2010) A neural basis for motor primitives in the spinal cord. J Neurosci 30:1322–1336

Haruno M, Wolpert DM (2005) Optimal control of redundant muscles in step-tracking wrist movements. J Neurophysiol 94:4244–4255

Imagawa H, Hagio S, Kouzaki M (2013) Synergistic co-activation in multi-directional postural control in humans. J Electromyogr Kinesiol 23(2):430–437

Jacobs R, van Ingen Schenau GJ (1992) Control of an external force in leg extensions in humans. J Physiol 457:611–626

Jones KE, Hamilton AFC, Wolpert DM (2002) Sources of signal-dependent noise during isometric force production. J Neurophysiol 88:1533–1544

Kouzaki M, Shinohara M, Masani K, Kanehisa H, Fukunaga T (2002) Alternate muscle activity observed between knee extensor synergists during low-level sustained contractions. J Appl Physiol 93:675–684

Kurtzer I, Pruszynski JA, Herter TM, Scott SH (2006) Primate upper limb muscles exhibit activity patterns that differ from their anatomical action during a postural task. J Neurophysiol 95:493–504

Kutch JJ, Valero-Cuevas FJ (2012) Challenges and new approaches to proving the existence of muscle synergies of neural origin. PLoS Comput Biol 8(5):e1002434

Kutch JJ, Kuo AD, Bloch AM, Rymer WZ (2008) Endpoint force fluctuations reveal flexible rather than synergistic patterns of muscle cooperation. J Neurophysiol 100:2455–2471

Lee DD, Seung HS (1999) Learning the parts of objects by non-negative matrix factorization. Nature 401:788–791

Masani K, Popovic MR, Nakazawa K, Kouzaki M, Nozaki D (2003) Importance of body sway velocity information in controlling ankle extensor activities during quiet stance. J Neurophysiol 90:3774–3782

Roh J, Rymer WZ, Beer RF (2012) Robustness of muscle synergies underlying three-dimensional force generation at the hand in healthy humans. J Neurophysiol 107:2123–2142

Roh J, Rymer WZ, Perreault EJ, Yoo SB, Beer RF (2013) Alterations in upper limb muscle synergy structure in chronic stroke survivors. J Neurophysiol 109(3):768–781

Takei T, Seki K (2010) Spinal interneurons facilitate coactivation of hand muscles during a precision grip task in monkeys. J Neurosci 30:17041–17050

Ting LH, Macpherson JM (2005) A limited set of muscle synergies for force control during a postural task. J Neurophysiol 93:609–613

Todorov E, Jordan M (2002) Optimal feedback control as a theory of motor coordination. Nat Neurosci 5:1226–1235

Torres-Oviedo G, Ting LH (2007) Muscle synergies characterizing human postural responses. J Neurophysiol 98:2144–2156

Torres-Oviedo G, Ting LH (2010) Subject-specific muscle synergies in human balance control are consistent across different biomechanical contexts. J Neurophysiol 103:3084–3098

Torres-Oviedo G, Macpherson JM, Ting LH (2006) Muscle synergy organization is robust across a variety of postural perturbations. J Neurophysiol 96:1530–1546

Tresch MC, Jarc A (2009) The case for and against muscle synergies. Curr Opin Neurobiol 19(6):601–607

Tresch MC, Saltiel P, Bizzi E (1999) The construction of movement by the spinal cord. Nat Neurosci 2(2):162–167

Vos EJ, Mullender MG, van Ingen Schenau GJ (1990) Electromechanical delay in the vastus lateralis muscle during dynamic isometric contractions. Eur J Appl Physiol 60:467–471

Zar JH (1999) Biostatistical analysis. Prentice-Hall, Upper Saddle River